B. Description of the GEOS-3 (Terra) Data Assimilation System

I. Description of GEOS-3 Subsystem Improvements

The Goddard Earth Observing System-Version 3 (GEOS-3) Data Assimilation System (DAS) is a major upgrade in all aspects of the system over the GEOS-2 DAS. The configuration of GEOS-3 with 1-degree horizontal resolution is defined as the Terra system and will usually be referred to as GEOS-Terra. The fundamental algorithms of GEOS-2 are described in the Algorithm Theoretical Basis Document (1996; ATBD-96). The specific implementations that define GEOS-3 are discussed here. The implementations relative to the earlier versions of the GEOS DAS include improved model physics and resolution, a new analysis scheme, a new online quality control, improved data pre-processing, and the use of more data types. In terms of the impact on the quality of the GEOS-3 data products, major contributions come from (1) using an interactive land surface model to improve the surface temperature over land masses, (2) assimilating Special Sensor Microwave/Imager (SSM/I)-based total precipitable water (TPW) retrievals to reduce tropospheric moisture bias over the oceans, and (3) increasing the model horizontal resolution to 1 degree latitude x 1 degree longitude. Details of the subsystem improvements are described in the following sections.

ATBD-96 can be found at

http://dao.gsfc.nasa.gov/

then “Publications,” followed by “Algorithm Theoretical Basis Document.”

I.1 Interactive land surface model

In ATBD-96 the incorporation of an interactive land-surface model was identified as a priority development to address a number of documented shortcomings of the early versions of the GEOS DAS. During the winter, for instance, surface temperatures were found to be much colder than observations (Schubert et al. 1995). Also the summertime specific humidity was overestimated, likely related to excessive latent heat (Bosilovich and Schubert, 1998). Consequently, the lifted condensation level was simulated much lower than observations, which could contribute to continental precipitation bias. In addition, in GEOS-1 the soil water was prescribed so that there was not a water balance at the continental surface, which introduces significant difficulties in scientific investigations (Arpe 1998; Bosilovich et al. 1999). To address these problems, the DAO began a comprehensive effort to incorporate a state-of-the-art land-surface parameterization into the GEOS general circulation model (GCM) and DAS and to develop a flexible off-line land data assimilation (e.g. the Off-line Land-surface Global Assimilation, OLGA) to investigate the assimilation of land-surface parameters. (Discussed in C.6 New Data / Land Surface)

The Mosaic Land Surface Model (LSM) (Koster and Suarez, 1996) has been incorporated and validated in the GEOS assimilation system. The LSM includes prognostic water and energy balances at the surface. While this introduces additional degrees of freedom in the model simulation and long-term assimilation (compared to prescribed soil water), the water will be

balanced at the surface. Furthermore, the LSM has a representation of land-surface heterogeneity. The Mosaic approach allows for 'tiles' of different surface type to occupy different fractions of the model grid box. However, the spatial distribution of the surface types is not included within the grid box. This facilitates the comparison of high resolution surface data with like simulated surface types.

Validation of the GEOS-Terra land-surface has proceeded along two major paths. First, a compilation of surface station data available from the National Climate Data Center (NCDC) provides nearly global coverage of near-surface meteorology. This allows systematic evaluation of how well near-surface conditions are represented when only the large-scale forcing is constrained by observations. Second, detailed field experiment data (e.g. FIFE, Cabauw Netherlands, and ARM-SGP) include observations such as the turbulent heat fluxes, soil temperature, soil water and radiation that are critical to the LSM simulation. Even though it is difficult to rigorously link the global-scale model with these regional observations, much can be learned about the LSM comparison with point data (e.g. Betts et al. 1996, 1998).

The land-surface temperature is a critical parameter for the instrument teams using GEOS data. The cold winter bias in the GEOS-1 DAS proved to be detrimental to the CERES team. The Mosaic LSM surface parameterization has provided a substantial improvement of the pervasive cold northern hemispheric continental cold bias evident in the top panel of Figure 1. In the best-observed regions, over the United States and western Europe, the temperatures are very close to the independent measurements and comparable to the products from other centers. In Siberia, there is some indication of a warm bias in the GEOS-3 product, which is, again, consistent with the products from the other centers and points out a challenge for future development.

The comparison with the ARM data, Figure 2, shows that the diurnal cycle has been substantially improved. Without the LSM the temperature at night was too low, and the peak-to-peak daily variability was overestimated. Also shown are similar quantities from ECMWF. In the top panel, the two assimilated data products are closer to each other that to the station observations. While both analyses represent the transition from a more erratic to a more regular variability, as observed from 11-16 January (top panel), the details of the variability in the earlier part of the record are different. The validation of the Mosaic LSM in the GEOS Terra DAS continues with the investigation of the annual cycle and summer time data. Given the turnaround time in the assimilation, these results are pending. However, preliminary simulations and assimilations of the summertime are encouraging.

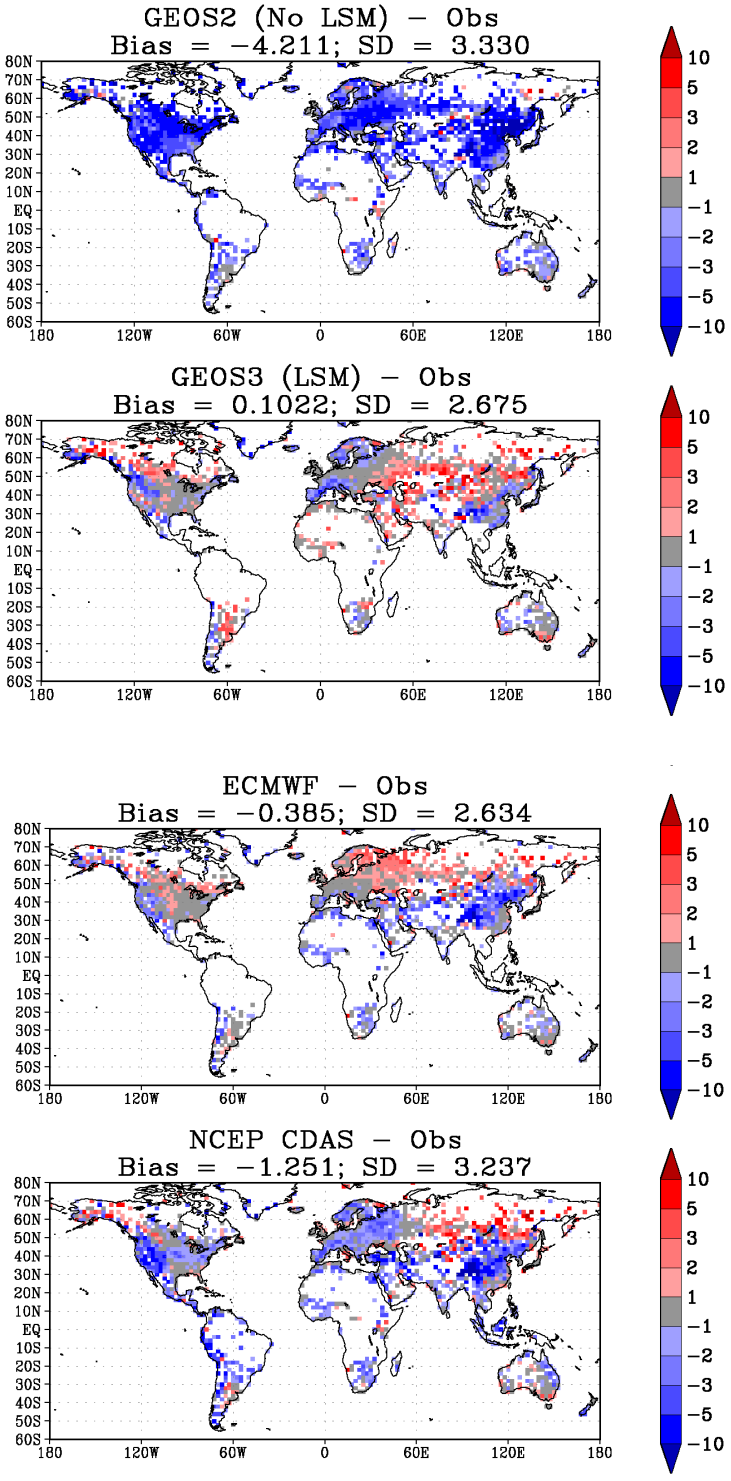

Figure 1: Near-surface temperature (K) difference between various assimilation systems and a collection of global stations for January 1998 in order from top to bottom, GEOS-2 without LSM, GEOS-3 with Mosaic LSM, ECMWF Reanalysis and NCEP CDAS. (2° x 2.5°)

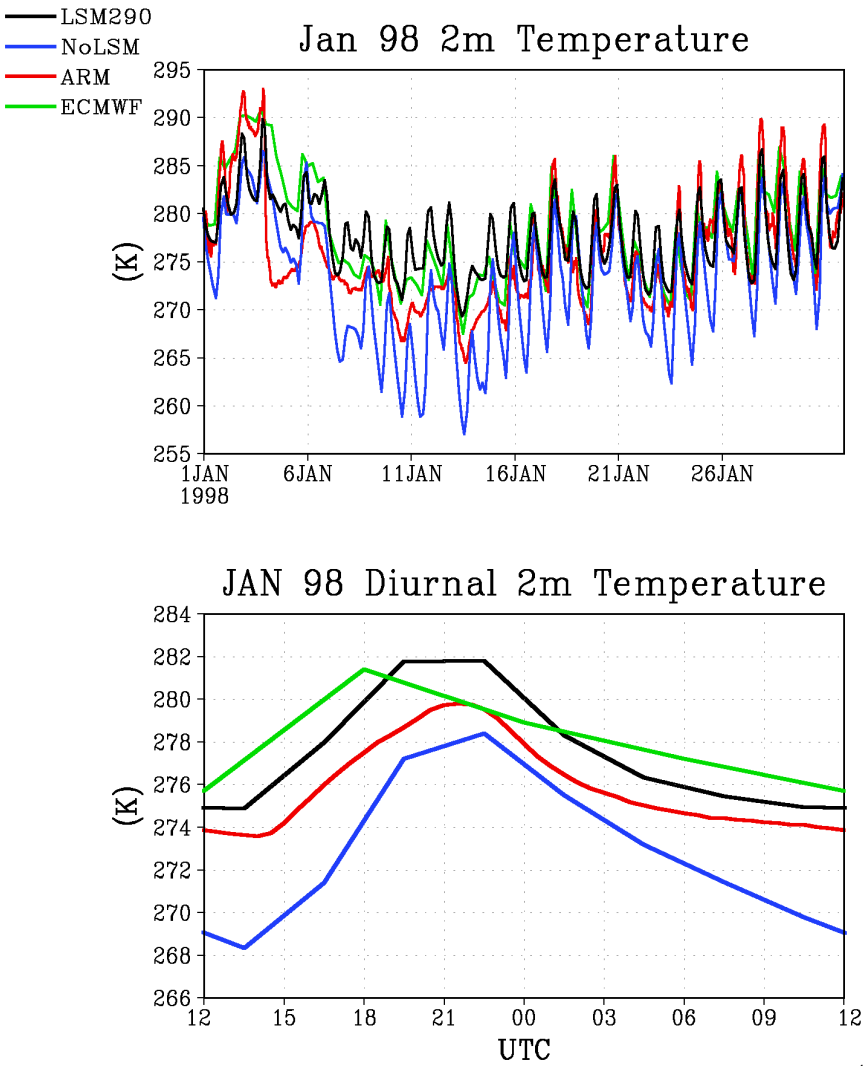

Figure 2: Time series of near surface temperature for January 1998 assimilation systems and the monthly mean diurnal cycle. LSM290 indicates the Current GEOS-Terra system, No LSM is GEOS-2 without the Mosaic LSM, ECMWF reanalyses data are included for comparison and the ARM data are from the central facility station.

I.2. Moist turbulence scheme

The deepening of the planetary boundary layer (PBL) can be driven not only by thermal convection from the earth's surface, but also by the buoyancy generated by the condensation and evaporation within shallow cumulus or stratocumulus convective clouds that sometimes occur near the top of the PBL. The level 2.5 second-order, turbulence closure scheme of Helfand and Labraga (1988) has been modified in the GEOS-3 DAS, following the work of Deardorff and Sommeria (1977) and Mellor (1977), to take this subgrid-scale condensation and evaporation into account. This "moist turbulence scheme," has resulted in deeper, more realistic simulations of the PBL within the DAS, especially over oceanic regions where boundary-layer clouds are the most likely to occur. Biases between assimilated PBL depths and those observed by NASA's Laser in Space Technology Experiments (LITE) instrument have been reduced significantly (Figure 3). There have also been improvements in the assimilation of vertical profiles of moisture within the lower atmosphere and of the vertical flux of heat and moisture near the top of the PBL. Low-level (below 700 hPa) cloud cover from the assimilation has improved dramatically in the tropics and subtropics (Figure 4), increasing from near zero to amounts comparable in magnitude and pattern to the observed climatology from the International Satellite Climatology Project (ISCCP).

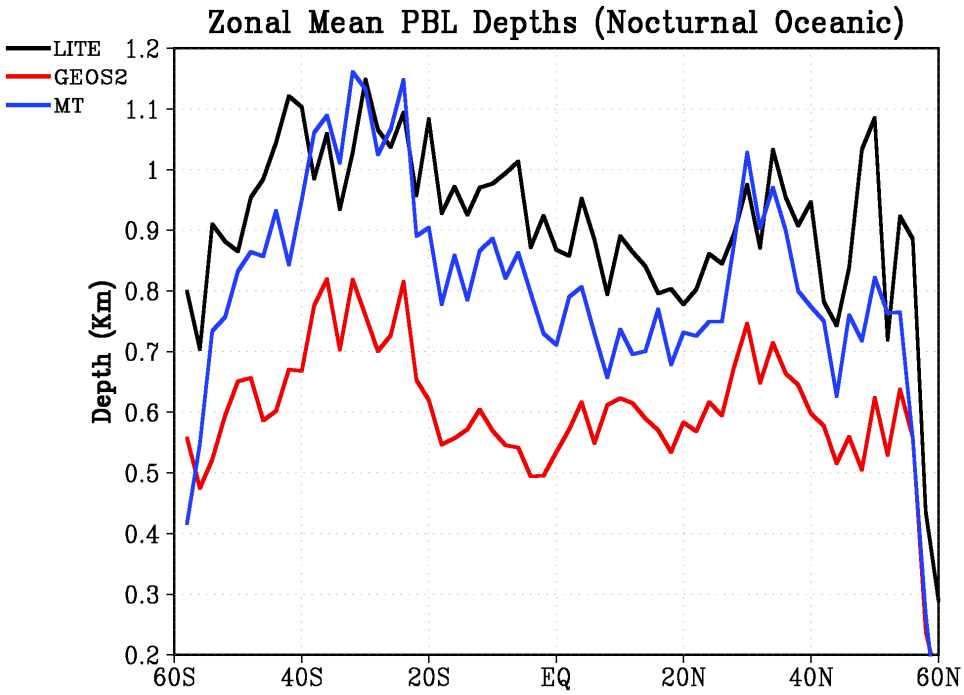

Figure 3: averaged planetary boundary layer depths (nocturnal and oceanic data only) for the period 10 - 19 September, 1994 for LIDAR In-space Technology Experiment (LITE) observations, GEOS-2 data assimilation, and GEOS-2 data assimilation including moist turbulence (MT) processes

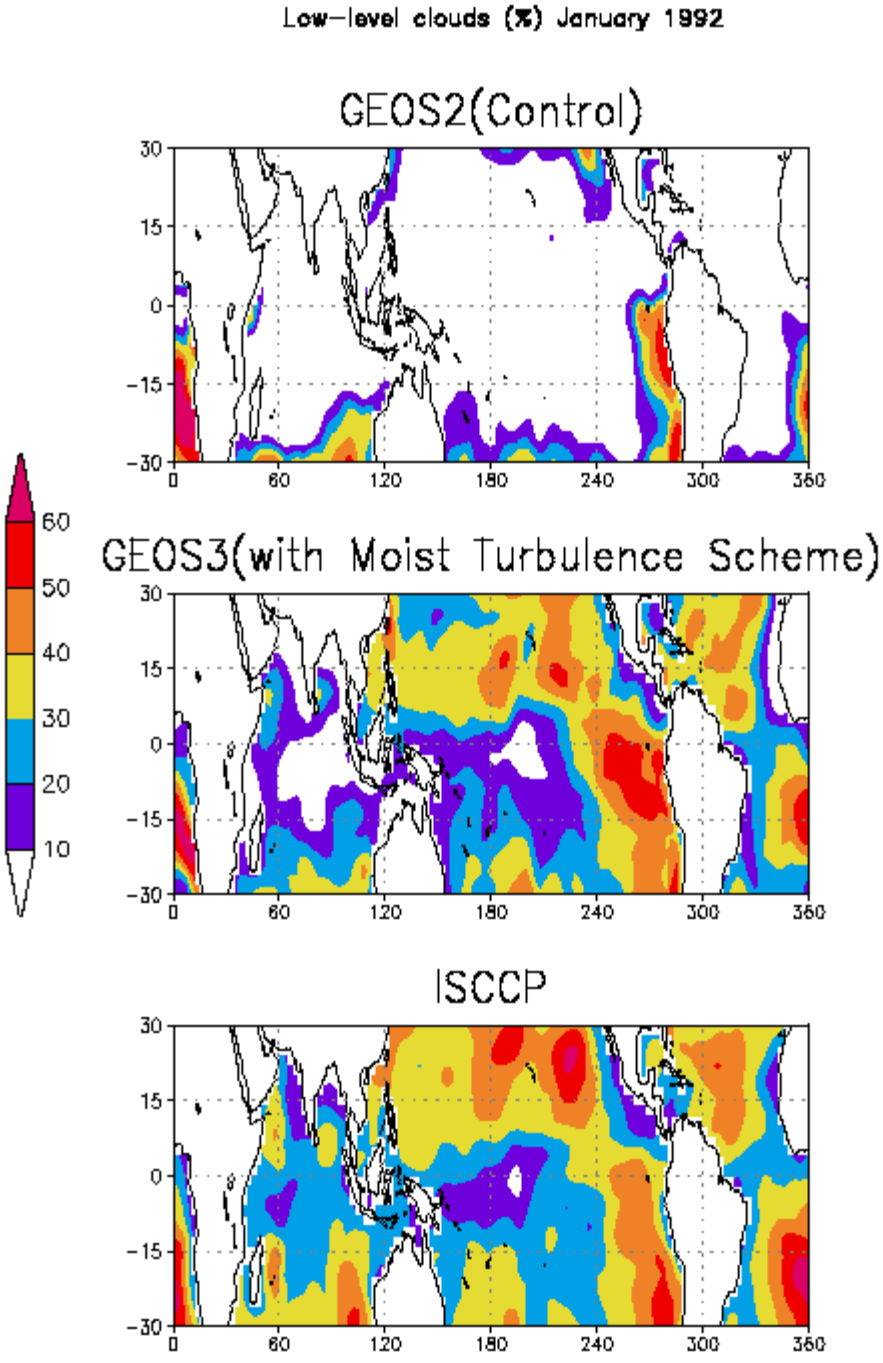

Figure 4: Implementation of the moist turbulence scheme dramatically improves the low cloud fraction in the GEOS-3 DAS as verified with ISCCP observations.

I.3. Increasing the model resolution to 1degree latitude by 1 degree longitude

The DAO has traditionally used grid-point models. Much of the motivation for using a grid-point has been the need to assure a good representation of tracer transport, which is often characterized by local structures related to shear in the wind field. Grid-point schemes are, by nature, more local than spectral schemes, and as discussed in Lin and Rood (1996) the non-local nature of the spectral schemes has a significant negative impact on comparisons of tracer simulations with tracer observations. The GEOS-3 model, used in the GEOS-Terra product, is a traditional grid point model. The next-generation model discussed in Section D.1 is a finite-volume model that maintains the local nature of the grid-point model, while increasing the accuracy and the physical consistency of the model substantially.

One might expect that the increased resolution would improve the model's ability to simulate fronts in a more realistic fashion, and that the ability to resolve local features will be more consequential in grid-point than in spectral models. Increased resolution of the GEOS GCM has provided substantial advances in the ability to simulate the structure and evolution of cyclones and fronts. Figure 5 illustrates the near surface wind fields derived from a three-month simulation using the GOES-3 GCM at two different horizontal resolutions. The top panel shows the simulation of cyclones and fronts over the North Atlantic using a uniform grid of 2 degrees latitude by 2.5 degrees longitude. At this resolution, fronts are represented as very broad transition zones and are barely discernible. The bottom panel shows the simulation for the same region using the GEOS-3 GCM with a uniform grid resolution of 1 degree in latitude and longitude. This simulation depicts a dramatic improvement over the coarser model results and illustrates a cyclone family along the Polar Front very clearly. At this resolution, the GEOS-3 GCM routinely displays remarkable agreement with both classical synoptic models and regional models of much higher resolution (25 km). In some cases, the GEOS-3 1x1 GCM produces extratropical cyclones that conform to the Shapiro-Keyser cyclone model, in other cases to the Norwegian frontal cyclone model. Case studies depict occurrences of occlusion, bent-back warm fronts, frontal fracture, frontal T-bone, and warm core seclusion (Conaty et al. 1999).

The impact of the 1x1 model resolution on the GEOS-Terra analysis is shown in section II.3.

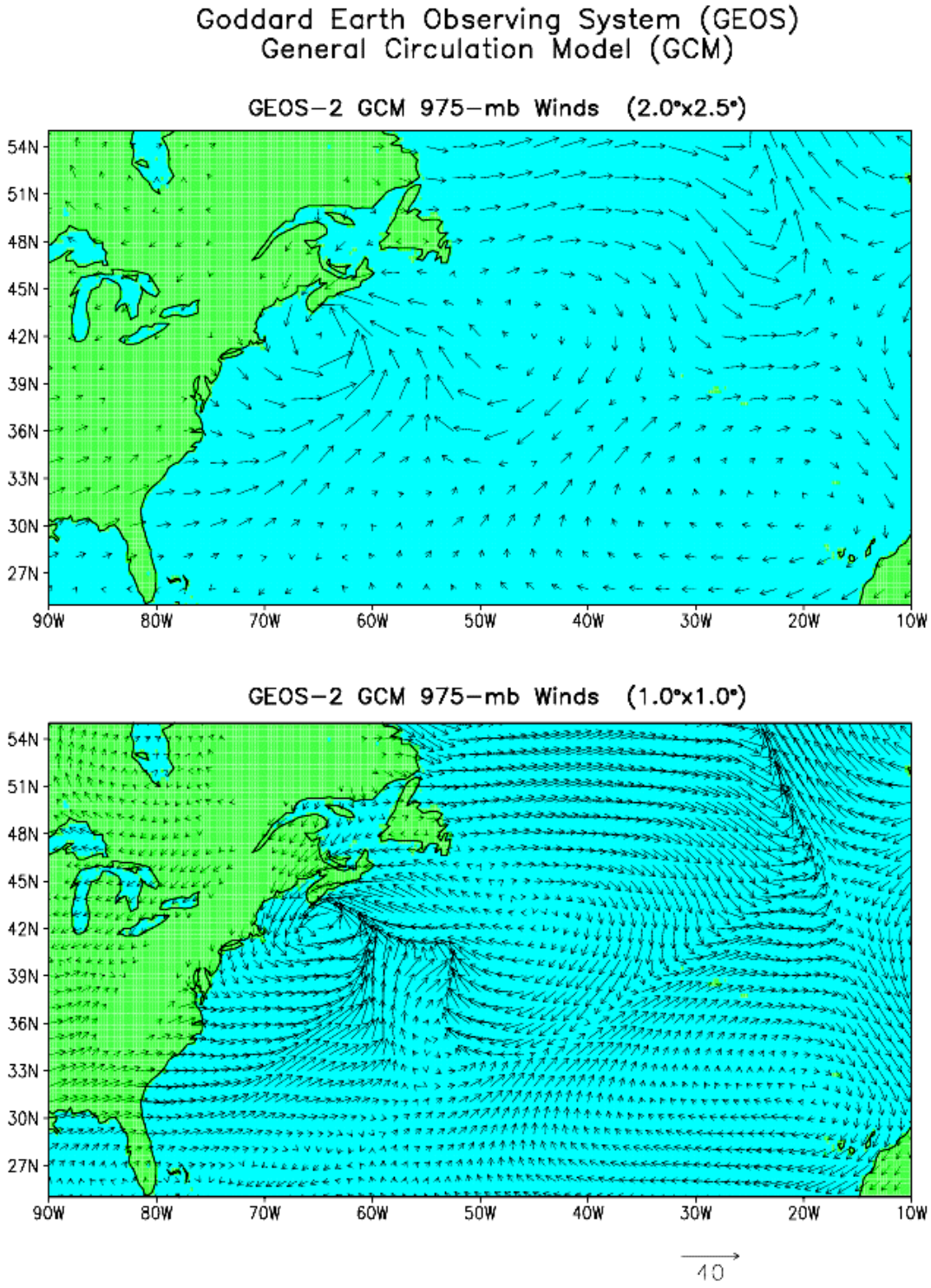

Figure 5: The top figure shows the simulation of cyclones and fronts using a uniform grid of 2 degrees latitude by 2x5 degrees longitude. The bottom figure shows the simulation for the same region using a uniform grid of 1 degree latitude by 1 degree longitude.

I.4. The Physical-space Statistical Analysis System (PSAS)

The Physical-space Statistical Analysis System (PSAS) is the data analysis component of the GEOS-3 DAS. It is a global three-dimensional variational (3D-Var) analysis system, much like the global spectral 3D-Var analysis systems that have replaced Optimal Interpolation (OI) analysis systems at the major numerical weather prediction centers over the last several years. PSAS differs from spectral 3D-Var systems in that it is formulated directly in physical space. The scientific rationale of PSAS, including comparison and contrast with spectral 3D-Var systems, is documented in ATBD-96 (Sec. 5.2). Also described there is the algorithmic formulation of PSAS, including the computational algorithm, the suite of parameterized error covariance models, and the covariance parameter tuning methodology. The scientific improvement of an experimental version of PSAS over its predecessor GEOS-1 OI system, in particular an improved analysis of the divergent component of the wind, was documented in Cohn et al. (1998).

The purpose of this section is to summarize briefly the major specific choices made in the current (GEOS-3) implementation of PSAS, from amongst the general options described in ATBD-96 (Sec. 5.2). Technical documentation of this implementation, including the computational algorithm, the factored operator covariance formulation, and the software implementation, is given in da Silva and Guo (1996), Guo et al. (1998), and Larson et al. (1998), respectively.

The choices are as follows:

The single-level univariate correlation model was chosen to be the Hadamard product of the powerlaw function (ATBD-96, Eq. 5.58) and the compactly-supported fifth-order piecewise rational function (ATBD-96, Eq. 5.60). This choice of model, described in detail in Gaspari and Cohn (1999, Sec. 4d), was found to give a good fit to data, keeps the computational cost of PSAS well within operational restrictions, and also happens to agree closely with the univariate model used by ECMWF (Rabier et al., 1998), which was developed through a different methodology.

The non-separable, multi-level univariate correlation model (ATBD-96, Eq. 5.64) was chosen to be the arithmetic mean of the single-level models, as described by Dee and da Silva (1999, Eq. 9). This simple choice was made to keep computer memory costs low, and was judged to be adequate for the GEOS-3 implementation as noted below. This model is non-separable in the sense that the horizontal correlation length varies in the vertical. More general, non-separable, multi-level correlation models have been formulated for PSAS, but are not implemented in GEOS-3.

An improved wind/mass balance was implemented, primarily by altering the parameterization of the height-coupled wind error model (ATBD-96, Eqs. 5.88, 5.89) in two ways. First, the geostrophic coupling was made to vary more smoothly with latitude, while keeping a smooth vertical dependence of the transition latitude, in better agreement with time-series of model climate statistics as well as time-series of 48h-24h forecast residuals. Second, a small explicit boundary-layer friction term was added to better represent frictional inflow into cyclones and outflow from anticyclones. The height-decoupled wind error variances (ATBD-96, Eqs. 5.91, 5.92) were also increased beyond the

values determined initially by maximum-likelihood tuning, in order to give more appropriate values to the total (coupled plus decoupled) wind error variances in the tropics.

Maximum-likelihood covariance parameter tuning has been carried out for the observation and forecast error covariance parameters, as described in ATBD-96 (Sec. 5.2). The scientific basis and many results of this parameter estimation process are given in Dee and da Silva (1999) and Dee et al. (1999), respectively. For some of the covariance parameters that are analogous between the GEOS-3 PSAS and the earlier OI system, considerably different values were found with the maximum-likelihood tuning. This fact, combined with the somewhat more flexible error covariance modeling allowed by the PSAS methodology, has contributed to a number of product improvements.

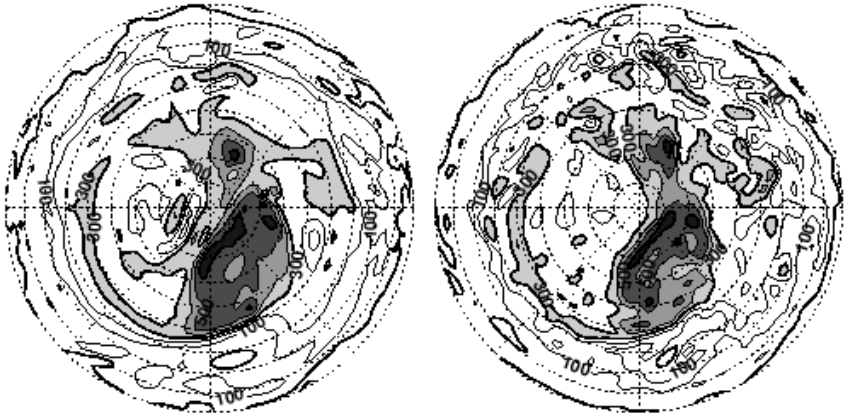

Figure 6: Northern hemisphere plot of 10 hPa potential vorticity at 12UTC 10 January 1998 from data assimilation systems based on PSAS (left panel) and OI (right panel). The equal-area projection extends from the equator to the pole with dotted lines every 10 degrees latitude. The Greenwich meridian is at 3 o'clock. Contour levels are every 100 PV units.

As one illustration, in Figure 6 is shown the 10hPa potential vorticity analysis at 12UTC on 10 January 1998, with the PSAS result on the left and the corresponding OI result on the right. The PSAS field on the left shows a smooth, well-formed polar vortex with several filaments. The OI field on the right introduces unrealistic small-scale features that distort the vortex and disrupt the filamentary structures. Three factors contributed to the improved PSAS potential vorticity field. First, most of the noisiness in the right panel between 20 N and 30 N is removed in the left panel by the smooth geostrophic decoupling of the PSAS height-coupled wind error covariance model. Second, the non-separable formulation of the PSAS multi-level height forecast error covariance model results in smooth, fairly large-scale analysis increments at this level. Third, the shorter vertical correlation length scales resulting from the maximum-likelihood tuning prevents rawinsonde observations from levels well below 10hPA, which contributed some of the spurious small-scale features in the OI case, from having any influence at all in PSAS analysis at 10 hPa.